



Contents lists available at ScienceDirect

Journal of Power Sources

journal homepage: www.elsevier.com/locate/jpowsour

Modulation on charge recombination and light harvesting toward high-performance benzothiadiazole-based sensitizers in dye-sensitized solar cells: A theoretical investigation

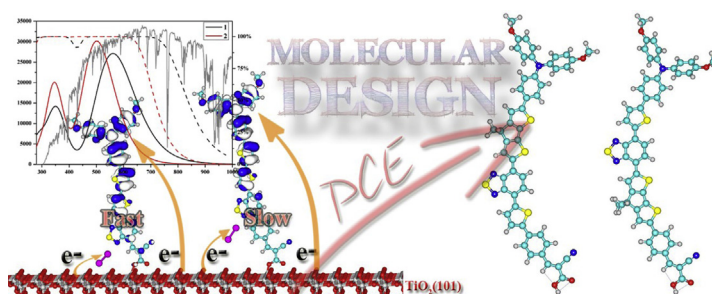
Jian-Zhao Zhang, Ji Zhang, Hai-Bin Li, Yong Wu, Hong-Liang Xu, Min Zhang*, Yun Geng*, Zhong-Min Su*

Institute of Functional Material Chemistry, Faculty of Chemistry, Northeast Normal University, Chang Chun 130024, Jilin, PR China

HIGHLIGHTS

- The different performance of reported dyes was rationalized by DFT calculations.
- Present a comprehensive strategy to design high-efficiency dye.
- Designed dyes **6** and **7** are promising candidates to further improve efficiency.

GRAPHICAL ABSTRACT



ARTICLE INFO

Article history:

Received 1 March 2014

Received in revised form

16 May 2014

Accepted 17 May 2014

Available online 28 May 2014

Keywords:

Benzothiadiazole

Triphenylamine-based organic dyes

Dye sensitized solar cells

Charge recombination

Time-dependent density functional theory

ABSTRACT

Factors associated with short circuit current density (J_{sc}) and open circuit photovoltage (V_{oc}) of dye sensitized solar cells (DSSCs) have been analyzed through DFT and TDDFT calculations to explore the origin of the significant performance differences with only tiny structure difference (1.24% for **1** and 8.21% for **2**) (Advanced Functional Materials 2012, 22, 1291–1302). Our results reveal that the insertion of phenyl ring in **2** enlarges the distance between the dye cation hole and the semiconductor surface and makes the benzothiadiazole (BTDA) unit, which has strong interaction with the electrolyte, far away from the semiconductor, resulting in a decreased charge recombination rate compared with that of **1**. However, the insertion of phenyl ring also results in a distortion of the molecular structure, leading to a decreased light harvesting ability. Hence, two dyes (**6** and **7**) derived from **2** with better conjugation degree, farther position of BTDA unit and longer molecular length have been designed to keep the advantages and overcome the disadvantages of **2** simultaneously. The results demonstrate that we get the desired properties of dyes through reasonable molecular design, and these two dyes could be promising candidates in DSSC field and further improve the performance of the cell.

© 2014 Elsevier B.V. All rights reserved.

1. Introduction

As one of the most promising renewable energy devices, dye sensitized solar cells (DSSCs) are receiving tremendous attention due to their low production costs, good flexibility, light weight and easy production processes [1–6]. Up to now, the overall power

* Corresponding authors. Tel.: +86 0431 85099291; fax: +86 431 85684009.
E-mail addresses: zhangm914@nenu.edu.cn (M. Zhang), gengy575@nenu.edu.cn (Y. Geng), zmsu@nenu.edu.cn (Z.-M. Su).

conversion efficiency (PCE, η) of DSSCs has reached 13.0% [7] reported by Grätzel and co-workers [8], however, which is still lower than that of the traditional Si-based solar cells [9]. Thus, lots of researches are still devoted to improving the PCE of DSSCs [1,8,10–16]. Generally, a typical DSSC is mainly composed of semiconductor material, dye sensitizer and electrolyte. There is no doubt that the development of new efficient sensitizers is an effective way to enhance the efficiency of DSSCs in view of the key roles of the sensitizer played in the cell, such as affecting the lighting harvesting efficiency, the charge transfer process and ultimately the PCE of the cell.

Currently, there are mainly three kind of dyes commonly used in DSSC [2], including ruthenium dyes [16–18], porphyrin dyes [19,20] and metal-free organic dyes [21–23]. Compared with the other two types of dyes, organic D- π -A dyes have received an ever-increasing attention due to their lower cost, easy of fabrication, relative higher molar extinction coefficients and environmental friendly. Impressively, the efficiency of DSSC based on champion organic dye (C219) is up to 10.3% [24]. However, organic dyes also have their own drawbacks such as the narrower absorption spectrum, and the faster

charge recombination due to the presence of the heteroatom [25]. Thus, great efforts have been devoted to the design and optimization of novel dyes to overcome these shortcomings [26–33]. For example, Haid et al. synthesized two triphenylamine-based (TPA) organic dyes [34] with tiny structure difference, as shown in Fig. 1. It is found that the insertion of phenyl ring between the benzothiadiazole (BTDA) unit and the cyanoacrylic acid group of **2** can lead to a 6.5 fold increase in cell efficiency (1.24% for **1** and 8.21% for **2**) [34]. How could this happen? In this paper, our initial interest focused on exploring the physical origin of the performance difference based on two organic dyes only with tiny structure difference. Here, in order to shed light on the reason of the performance difference, key parameters including open circuit photovoltage (V_{oc}) and short circuit current density (J_{sc}) were systematically investigated in detail based on density functional theory (DFT) and time-dependent DFT (TDDFT) calculations. In addition, we also designed two dyes (**6** and **7**) with stronger light harvesting ability and slower charge recombination, which will be potential sensitizers for DSSCs. We hope our work can provide guidance to the design of new dyes and will move the DSSCs field forward.

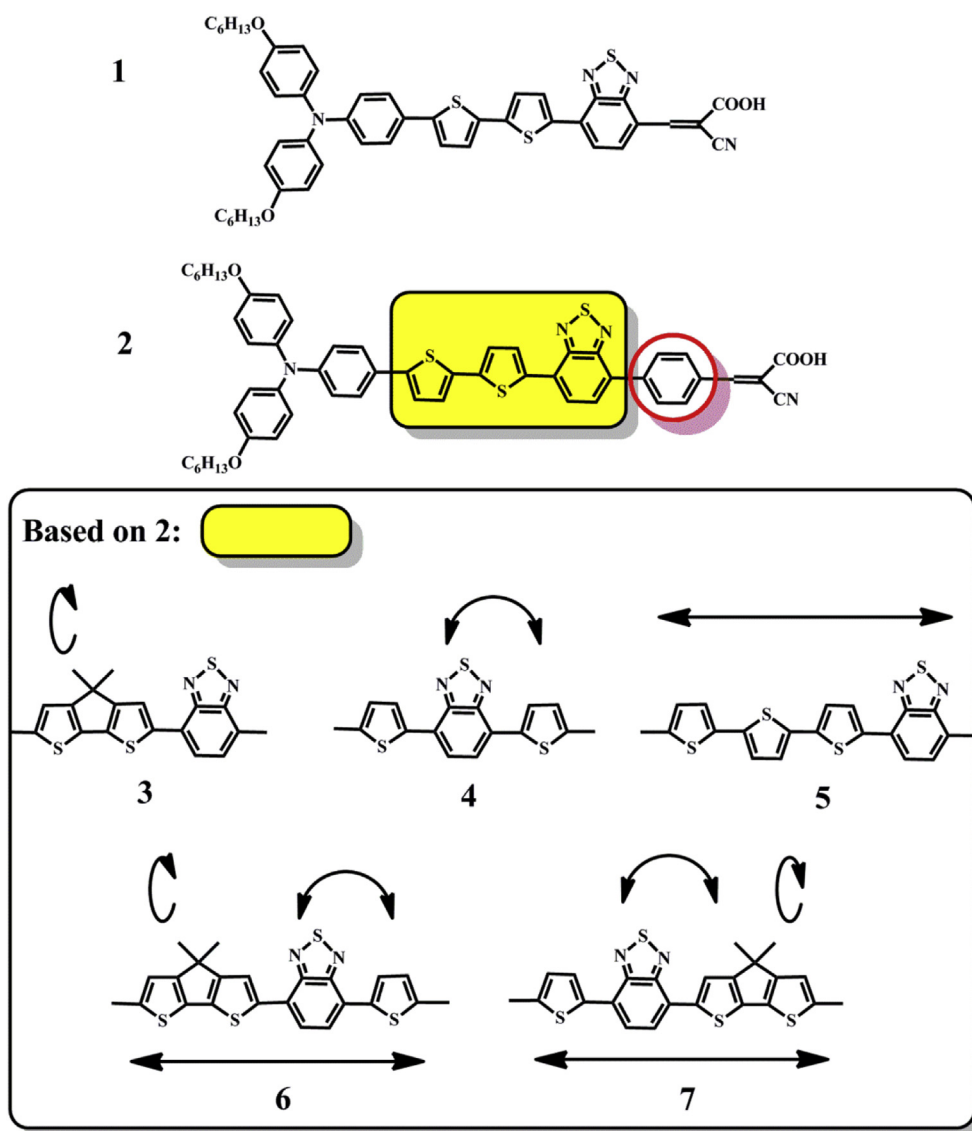


Fig. 1. The structures of studied organic dyes.

2. Computational details

All the calculations are performed in Gaussian09 code [35] at DFT and TDDFT level. The ground state molecular structures of dyes under study were optimized at B3LYP/6-31G(d) level, followed by frequency calculations to make sure we got stable structures [36]. The absorption spectra were calculated at CPCM/CAM-B3LYP/6-31G(d) level considering real solvent effect (dichloromethane) with conductor-like polarizable continuum model [37] and the long-range correction [38]. To evaluate the extent of charge recombination process between dyes and electrolyte, we also calculated the interaction energy between dye and I_2 with M06-2X functional [39–41], which is considered as a suitable functional for the description of weak interaction, together with 6-31G(d) basis set for C, H, N, O, S and LANL2DZ basis set and corresponding effective core potential for I atom. And, the counterpoise method was used to compensate the basis set superposition error (BSSE) [42,43].

For the semiconductor surface effects, we take $(TiO_2)_{38}$ cluster [44] obtained by cutting an anatase slab primarily exposing the 101 surface into consideration as shown in Fig. S1, because this surface has been demonstrated to be the most stable and typically observed surface for this material [45,46]. De Angelis and co-workers also found that the excitation energy of $(TiO_2)_{38}$ cluster is in good agreement with the experimental results of the TiO_2 semiconductor [47,48]. Thus we believe that it is reasonable to use this model to simulate the effects of the semiconductor surface. The structures of dyes binding to the $(TiO_2)_{38}$ cluster in vacuum was optimized by SIESTA code [49–51], and the computational details are listed in SI (Supporting information). Besides, the Density of States (DOS) profiles used to estimate the change of conduction band energy level was obtained at C-PCM/B3LYP/SVP level [52].

3. Results and discussion

The PCE of the cell has a close relationship with the J_{sc} , V_{oc} and the fill factor (FF). And it can be estimated as [53]:

$$\eta = \frac{P_{max}}{P_{in}} = FF \frac{V_{oc} J_{sc}}{P_{in}} \quad (1)$$

where P_{max} and P_{in} are the maximum and incident power of the DSSCs, respectively.

As discussed in the part of the introduction, we know that **1** and **2** synthesized by Haid et al. [34] with tiny structure difference have significant different photovoltaic performance data (J_{sc1} : 3.40 mA cm⁻², V_{oc1} : 489 mV, FF₁: 0.74; J_{sc2} : 18.47 mA cm⁻², V_{oc2} : 640 mV, FF₂: 0.69). Thus in order to get a deep understand on the essential reasons of the significant difference in η of the solar cells based on these two dyes from the theoretical point of view, we will analyze how the molecular structure of the sensitizer affects the J_{sc} and V_{oc} .

3.1. Theoretical explanations for the V_{oc} difference

For V_{oc} in DSSCs, it can be determined by [54]:

$$V_{oc} = \frac{E_{CB} + \Delta CB}{q} + \frac{k_B T}{q} \ln \left(\frac{n_c}{N_c} \right) - \frac{E_{redox}}{q} \quad (2)$$

here, E_{CB} is the conduction band energy level, ΔCB is the shift of the conduction band energy level. n_c is the number of the electrons in the conduction band of semiconductor, N_c is the electron density of state, E_{redox} is the oxidation potential of the redox couple in the electrolyte, k_B is the Boltzmann constant, T is the temperature, q is

the unit charge. It is obvious that ΔCB and n_c are the factors which could change the V_{oc} of the cell. In fact, a large number of theoretical and experimental investigations [55–60] have demonstrated that for the cells under the same experimental conditions with just different sensitizers, the main reason for the V_{oc} difference is the different ΔCB and different extent of charge recombination affecting n_c .

Actually there are many factors could induce ΔCB , such as, solvent, ions in the electrolyte and dye sensitizers. The express is presented as follows [56,58,59]:

$$\Delta CB_{tot} = \Delta CB_{solv} + \Delta CB_{ions} + \Delta CB_{dye} \quad (3)$$

ΔCB_{tot} means total TiO_2 conduction band shift, ΔCB_{solv} , ΔCB_{ions} and ΔCB_{dye} represent the shifts induced by the solvent, ions and adsorbed sensitizer in electrolyte, respectively. However, under the same experimental condition, ΔCB_{solv} and ΔCB_{ions} could be considered as the constant. Thus it is easy to get a conclusion that the conduction band energy shift of dye sensitizer has a significant effect on the ΔCB_{tot} and finally have an important influence on V_{oc} based on Eq. (2).

For another important factor affecting the performance of the cell from the sensitizers point of view, it is the charge recombination as described above, which could affect n_c . There are mainly two charge recombination processes in the solar cell, one is the recombination between the injected electrons and dye cation (k_{rec1}), and the other is that between the injected electrons and electrolyte (k_{rec2}). Detailed descriptions are listed as follows:

$$k_{rec} = k_{rec1} + k_{rec2} \quad (4)$$

Based on the electron-transfer theory [61–63], k_{rec1} could be expressed as [64]:

$$k_{rec1} = \frac{H_{AB}^2}{\sqrt{4\pi\lambda k_B T}} \exp \left(- \frac{(\Delta G^0 - \lambda)^2}{4\lambda k_B T} \right) \quad (5)$$

$$H_{AB}^2 = H_0^2 e^{-\beta r} \quad (6)$$

H_{AB}^2 , ΔG^0 are the electron coupling and the free energy between the donor and acceptor states, respectively, and λ is the reorganization energy. For the H_{AB}^2 , it is related to electron tunnelling through a potential barrier (β , which is a function of the barrier height of intervening media) and shows an exponential increase with the increasing spatial distance (r) between donor and acceptor states. Obviously, k_{rec1} is determined by ΔG^0 , λ , β and r . Among the four parameters, λ is significantly controlled by the solvent, and β is associated with the intervening media, which means that they are not molecular control. Assuming all the DSSCs device are fabricated in same experiment condition, the λ and β would be same. In addition, for ΔG^0 , which is defined as the difference between the ground state oxidation potential of dyes and the Fermi level of semiconductor, Clifford et al. has demonstrated that k_{rec1} is not sensitive to the ΔG^0 [64]. Thus, we focus on the spatial distance r between donor and acceptor to estimate k_{rec1} . Here, donor is defined as the injected electron in the conduction band of semiconductor and acceptor as the dye cation hole (dye cation HOMO β orbital was used).

For the k_{rec2} , as we all know, the higher concentration of reactant is, the higher reaction rate is. Some experiments have revealed that some atoms or groups could provide binding sites for iodine through halogen bond [65–67], which would increase the local concentration of iodine in the vicinity of the semiconductor surface [60,68–72]. And De Angelis and co-workers have demonstrated that the more predominant interaction sites the dye has and the shorter distance between iodine and semiconductor surface is, the

larger the $k_{\text{rec}2}$ is [25,60]. And this strategy has been widely applied in theoretical research of DSSCs [57,58,73]. Thus, we calculated the interaction energy between dyes and iodine and the approximate distance between iodine and semiconductor surface to analyze $k_{\text{rec}2}$ qualitatively.

3.1.1. Molecular structure effects on the conduction band energy level shift, ΔCB

In order to get the conduction band energy shift induced by the adsorption of sensitizer, we firstly carried out full geometry optimization of dyes adsorbed onto TiO_2 surface using the preferred bidentate bridging mode with deprotonation after adsorption [74,75]. The optimized structures of dye/ $(\text{TiO}_2)_{38}$ are shown in Fig. 2. Then, based on the optimized geometries, the DOS profiles for TiO_2 with dyes and Partial Density of States (PDOS) profiles for pure TiO_2 at the B3LYP/SVP level in acetonitrile solvent were analyzed [56]. As shown in Fig. 3, the corresponding ΔCB for **1** and **2** are 0.263 eV and 0.256 eV, suggesting that **1** and **2** have similar shift in conduction band edge. What is the origin of conduction band shift? Actually, there are two effects proposed by Ronca et al. [56] when dye adsorbs onto the semiconductor. One is the charge transfer effect due to electron density

arrangement, and the other is the electrostatic effect due to the dipole moment. Thus, we also quantitatively estimate this two effects through the entity of charge transfer (q^{CT}) originated from the charge displacement curve and the average electrostatic potential (V_{EL}) generated by the molecular charges evaluated on the first layer of the TiO_2 cluster as shown in Table 1. The computational details should be found in the paper of Ronca et al. [56] and our previous works [58,73]. From Table 1, it is found that the q^{CT} of **1** and **2** are 0.38 and 0.36 respectively, and V_{EL} of them of all -0.21 . Obviously, the similar ΔCB should be owing to the similar q^{CT} and V_{EL} . In any case, it should be found that ΔCB is not the dominant factor resulting in the significant difference of V_{oc} between **1** and **2**. Thus, we discussed the charge recombination in the following in an attempt to rationalize the significant difference of V_{oc} .

3.1.2. Molecular structure effects on the charge recombination process, n_c

As mentioned above, n_c , which is closely associated with charge recombination including $k_{\text{rec}1}$ and $k_{\text{rec}2}$, also plays an important role in affecting V_{oc} . Therefore, in the following we will discuss how the molecular structure difference affect $k_{\text{rec}1}$ and $k_{\text{rec}2}$.

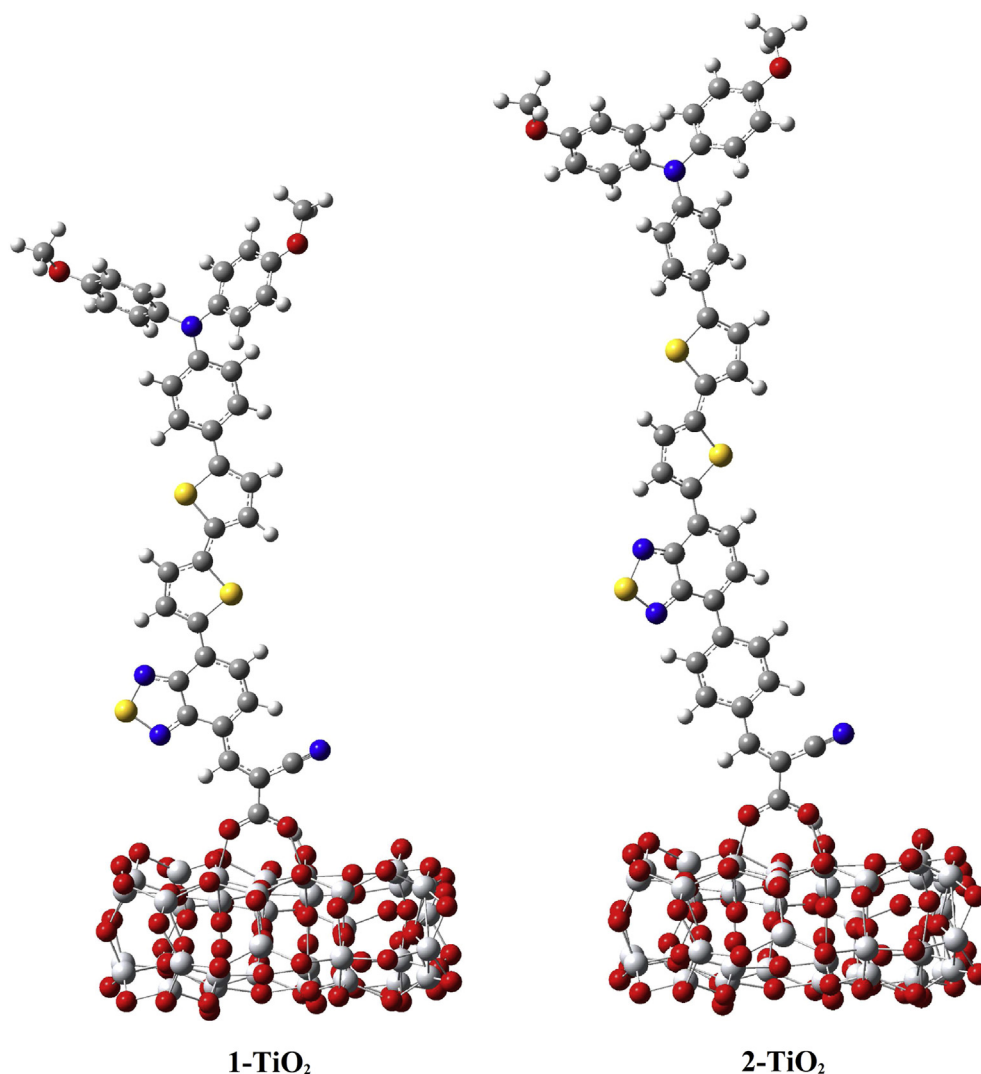


Fig. 2. The optimized molecular structures of **1**-(TiO_2)₃₈ and **2**-(TiO_2)₃₈ by SIESTA code.

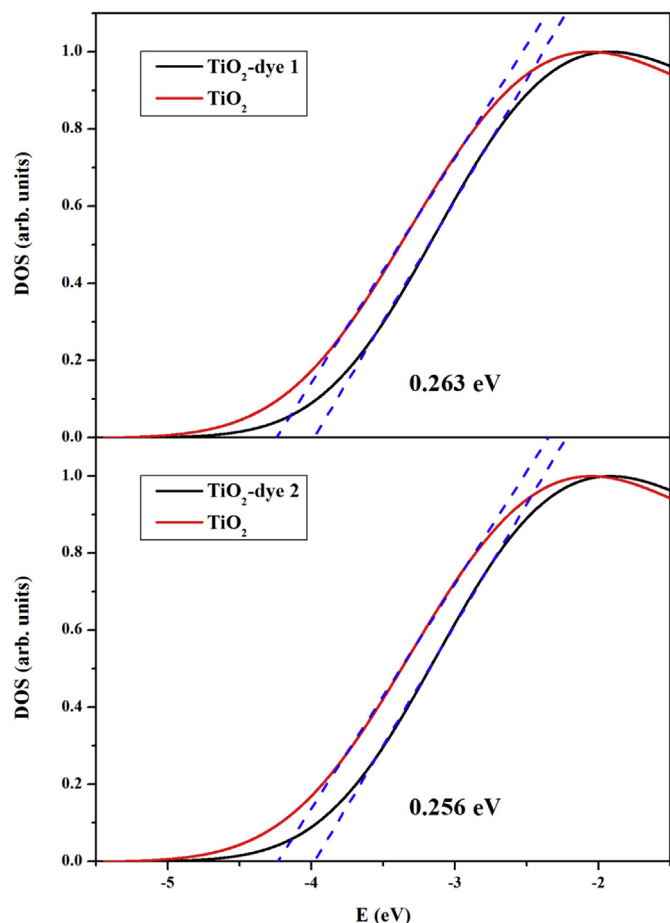


Fig. 3. Total and partial density of states (DOS) of 1-(TiO₂)₃₈ and 2-(TiO₂)₃₈.

As for k_{rec1} , it is mainly determined by the hole-surface distance r between donor and acceptor states according to the nonadiabatic electron transfer theory. Moreover, Durrant and his co-workers [64] also found that, in general, DSSCs employing smaller dyes exhibit faster k_{rec1} because of the shorter r between the dye cation hole and semiconductor surface. Thus, we followed their strategy and calculated the spatial distance r by multiplying the percentage contribution of each atom to the HOMO and the corresponding distance between the carbon atom of the carboxylic group and each atom of the dye cation to evaluate k_{rec1} . The results are shown in Fig. 4. From Eq. (6), we know that the H_{AB}^2 exhibits an exponential increase with respect to the distance r , the longer r , the larger H_{AB}^2 . Hence, the 3.6 Å lower of **1** on r than that of **2** could lead to significant decrease of k_{rec1} .

To analyze the extent of k_{rec2} of different dyes, the interaction energies between dye and I₂ and their corresponding approximated distances were calculated and shown in Fig. 5. We can see that, for **1**, it has three predominant sites, 1-N2 (−5.74 kcal mol^{−1}; 1.3 Å), 1-N3 (−5.67 kcal mol^{−1}; 7.1 Å) and 1-N1 (−5.65 kcal mol^{−1}; 10.1 Å), respectively, implying that I₂ prefer to surround the BTDA unit and CN group rather than the others. With respect to **2**, the predominant sites are at 2-N2 (−6.73 kcal mol^{−1}; 6.4 Å) and 2-N1 (−6.13 kcal mol^{−1}; 14.1 Å), also showing that BTDA unit has strong interaction with I₂. Compared **2** with **1**, following the conclusions of De Angelis and his co-workers, we believe that **2** has a smaller k_{rec2} than that of **1** because **2** has less predominant sites and each of the sites are farther than that of **1**. The calculated results suggest that BTDA unit could interact with I₂ strongly, and that the insertion of

phenyl ring could lead to the BTDA unit much farther away from the TiO₂ surface, which results in the k_{rec2} of **2** smaller than **1**. Obviously, BTDA units play important roles in controlling k_{rec2} .

It is worth mentioning that there are different kinds of dye-iodine complexes, such as dye-I₂ and I₃[−], and the dye-I₂ is the most important complex as its charge recombination rate is 2 order of magnitude faster than the dye-I₃[−] complex which was demonstrated by Green et al. [76], and this complex could accelerate k_{rec2} has also been observed in some related experiments [69,70,77]. In addition, there are some other factors could also affect the charge recombination process, such as the blocking effects induced by the alky chain on the sensitizer, the additive in the electrolyte, the thickness of the semiconductor and so on [2,78]. In our manuscript, these factors were not taken into consideration. Because for the DSSCs with just different sensitizers, we assume that they have the same experimental conditions, and we believe that the investigations for the inherent charge recombination of the sensitizers could be more important for the further optimization of the sensitizers. From the above discussion, taking both k_{rec1} and k_{rec2} into consideration, we found that it is the fast k_{rec} that lead to the lower V_{oc} of **1** than that of **2**, which is in agreement with the experiment [34]. And in the next, we will discuss how the molecular structures induce the J_{sc} difference.

3.2. Theoretical explanations for the J_{sc} difference

J_{sc} , as another key parameter determining the PCE of the cell, could be expressed as [53]:

$$J_{\text{sc}} = \int e \text{IPCE}(\lambda) I_{\text{s}}(\lambda) d\lambda \quad (7)$$

$$\text{IPCE}(\lambda) = \text{LHE}(\lambda) \Phi_{\text{inj}} \eta_{\text{coll}} \quad (8)$$

where IPCE(λ) is incident photon-to-current conversion efficiency at a fixed wavelength, which is the product of LHE(λ) (light harvesting efficiency at the certain wavelength), Φ_{inj} (electron injection efficiency) and η_{coll} (charge collection efficiency). And $I_{\text{s}}(\lambda)$ is the corresponding photon flux based on AM 1.5 G (global) solar radiation spectrum.

In terms of LHE(λ), it can be described by the following equation [79,80]:

$$\text{LHE}(\lambda) = 1 - 10^{-\epsilon(\lambda)bc} \quad (9)$$

here, $\epsilon(\lambda)$ is the molar absorption coefficient at certain wavelength, b is the thickness of film, and c is the concentration of dye. For discussing LHE(λ) conveniently, b and c are taken as 10 μm and 300 mmol L^{−1}, respectively [81,82].

For Φ_{inj} , it is related to the injection driving force (ΔG_{inj}) defined as the difference between the excited state oxidation potential of dye and the conduction band energy level of semiconductor. Thus, Φ_{inj} can be estimated qualitatively as follow [57,83–85]:

$$\Delta G_{\text{inj}} \propto k_{\text{inj}} \propto \Phi_{\text{inj}} \quad (10)$$

$$\Delta G_{\text{inj}} = E_{\text{dye}^*} - E_{\text{CB}} \quad (11)$$

$$E_{\text{dye}^*} = E_{\text{dye}} - \lambda_{\text{max}} \quad (12)$$

here, E_{dye^*} and E_{dye} are the excited and ground states oxidation potential, respectively. λ_{max} is the maximum absorption wavelength, E_{CB} is the conduction band energy level of semiconductor, and we adopted the experimental value −4.0 eV as our standard E_{CB}

Table 1

Calculated conduction band shift (ΔCB , eV), entity of charge transfer (q^{CT} , e), and average electrostatic potential on the first layer of TiO_2 cluster (V_{EL} , eV) for **1** and **2**.

Dye	ΔCB	q^{CT}	V_{EL}
1	0.263	0.38	−0.21
2	0.256	0.36	−0.21

in this paper [86]. Based the Eq. (10), we can estimate the Φ_{inj} by comparing the ΔG_{inj} .

As for η_{coll} , it is not only related to the electrode materials, but also have close relationship with the charge recombination process. In an ideal DSSC device, η_{coll} should be one. However, under the practical operation, η_{coll} can not reach 100% because of the charge recombination process. For the same semiconductor, the larger k_{rec} , the lower η_{coll} .

In addition, it is worth to note that light harvesting is not only associated with $\text{LHE}(\lambda)$, but also related to the absorption range. Thus, $I_s(\lambda)$ need to be taken into account when light harvesting is estimated according to Eq. (7) [53,79]. If we assume the unity efficiency for Φ_{inj} and η_{coll} , the calculated J_{sc} could be the theoretical maximum limit $J_{\text{sc}}^{\text{max}}$ which could quantitatively reflect the overall light harvesting ability of dyes, in other words, the matching degree between the absorption spectrum of the sensitizer and the photon flux spectrum.

As a result, it is obvious that the overall light harvesting ability (theoretical maximum limit $J_{\text{sc}}^{\text{max}}$), Φ_{inj} and η_{coll} are the key factors associated with the sensitizer affecting J_{sc} . And thus in the following, we will give a detailed interpretation for the difference of J_{sc} from these aspects.

3.2.1. Molecular structure effects on the light harvesting

In order to evaluate the overall light harvesting ability (theoretical maximum limit $J_{\text{sc}}^{\text{max}}$), we firstly calculated the maximum absorption wavelengths, vertical excitation energies, and nature of the transitions of the dyes under study and the results were summarized in Table 2. From Table 2, we can see that the maximum absorption peak for **1** and **2** is at 561 and 501 nm, respectively, both corresponding to the transition of S_0 to S_1 , which can be assigned as the promotion from HOMO to LUMO and HOMO-1 to LUMO. And the maximum absorption peaks are in good agreement with the experimental values (570 nm and 515 nm for **1** and **2**, respectively) [34], validating the rationality of our method and basis set we choosed. We also find that the insertion of phenyl ring could cause a

blue-shifted spectrum, resulting from the distortion of molecular structure of **2** as shown in Fig. S2. Inspection of the distribution of frontier molecular orbitals of **1** and **2** depicted in Fig. S3 shows that the HOMO-1s and HOMOs of both dyes are mainly located at TPA donors and thiophene rings, and the LUMOs are mainly located at BTDA units and cyanoacrylic acid groups, implying that the excited state transition (S_0 – S_1) is a charge-transfer transition.

To give an intuitive impression on light absorption, we simulated the UV/Vis absorption spectra of **1** and **2** shown in Fig. 6 through the Multiwfn code [87,88] at CPCM/TD-CAM-B3LYP/6-31G(d) level. As discussed above, we know that the theoretical maximum limit $J_{\text{sc}}^{\text{max}}$ is a really important factor affecting the J_{sc} of the cell, and it takes the absorption range, absorptance and the photon flux spectrum into consideration at the same time. Thus, according to Eqs. (7)–(9), we get the LHE curves and their corresponding $J_{\text{sc}}^{\text{max}}$ as shown in Fig. 6. The $J_{\text{sc}}^{\text{max}}$ of **1** and **2** are 29.83 mA cm^{-2} and 22.05 mA cm^{-2} , respectively, implying that **1** should have better overall light harvesting ability than that of **2** leading to a higher J_{sc} . Moreover, from the LHE curves, it could found that when the molar absorption coefficient at certain wavelength reaches some value, its corresponding $\text{LHE}(\lambda)$ will be close to one. And the larger $J_{\text{sc}}^{\text{max}}$ of **1** than that of **2** is mainly due to the red shift of the absorption. However, based on the experimental value, we know that the J_{sc} of dye **2** is far greater than that of dye **1**. The contrary tendency indicates that there must be some electronic loss processes in the whole circulation system of **1**-based DSSCs, causing that its J_{sc} was reduced rapidly. Thus, we will focus on the Φ_{inj} and η_{coll} , which are related to the electronic loss in the following.

3.2.2. Molecular structure effects on the electron injection efficiency (Φ_{inj}) and electron collection efficiency (η_{coll})

The driving force was used to evaluate the Φ_{inj} , and Islam et al. has demonstrated that when the injection driving force is above 0.2 eV, the Φ_{inj} will be unit [89]. Table 3 shows obviously that these two dyes have enough driving force to insure the photoexcited electron injection, which is in good agreement with the experiment data (Φ_{inj1} : 94.8%, Φ_{inj2} : 94.7%) [34]. Thus it is obvious that Φ_{inj} can not determine the difference in J_{sc} between two dyes. How does η_{coll} impact it?

The η_{coll} is mainly determined by k_{rec} , leading to the losing of injected electrons. From the Section 3.1.2, we know that the hole-surface distance r of **2** is larger and its predominant interaction site with I_2 is farther from the semiconductor surface due to the insertion of phenyl ring. Thus, we get a conclusion that the charge recombination between injected electron and dye cation (k_{rec1})/redox couple in electrolyte (k_{rec2}) of **2** are both smaller than that of **1**, leading to a higher η_{coll} of **2** than that of **1**. Thus, combining with their theoretical maximum limit $J_{\text{sc}}^{\text{max}}$, we believe that it is the lower η_{coll} of dye **1** than dye **2** that make the J_{sc} of DSSC based on dye **1** decrease.

From the above discussion about J_{sc} and V_{oc} , it can be clearly concluded that although **1** has better overall light harvesting ability (larger theoretical maximum limit $J_{\text{sc}}^{\text{max}}$), the J_{sc} , V_{oc} and η is lower than that of **2** due to the fast charge recombination, in good agreement with the experimental results [34]. It is the insertion of phenyl ring that lead to the decrease of k_{rec} . Our results also reveal that the charge recombination process plays an important role in affecting the J_{sc} , V_{oc} and η .

3.3. Further optimization through molecular design

Since we have known the main advantages and disadvantages of **2** through the above theoretical analysis and the comparison with the experimental results, these organic dyes (**3**–**5**) shown in Fig. 1

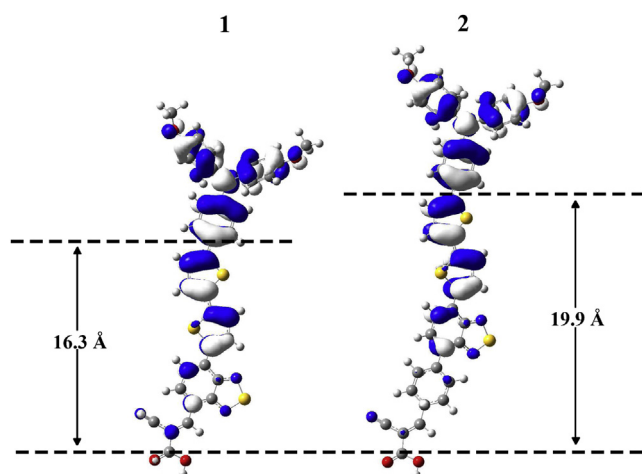


Fig. 4. The distance between dye cation hole and TiO_2 surface of **1** and **2**.

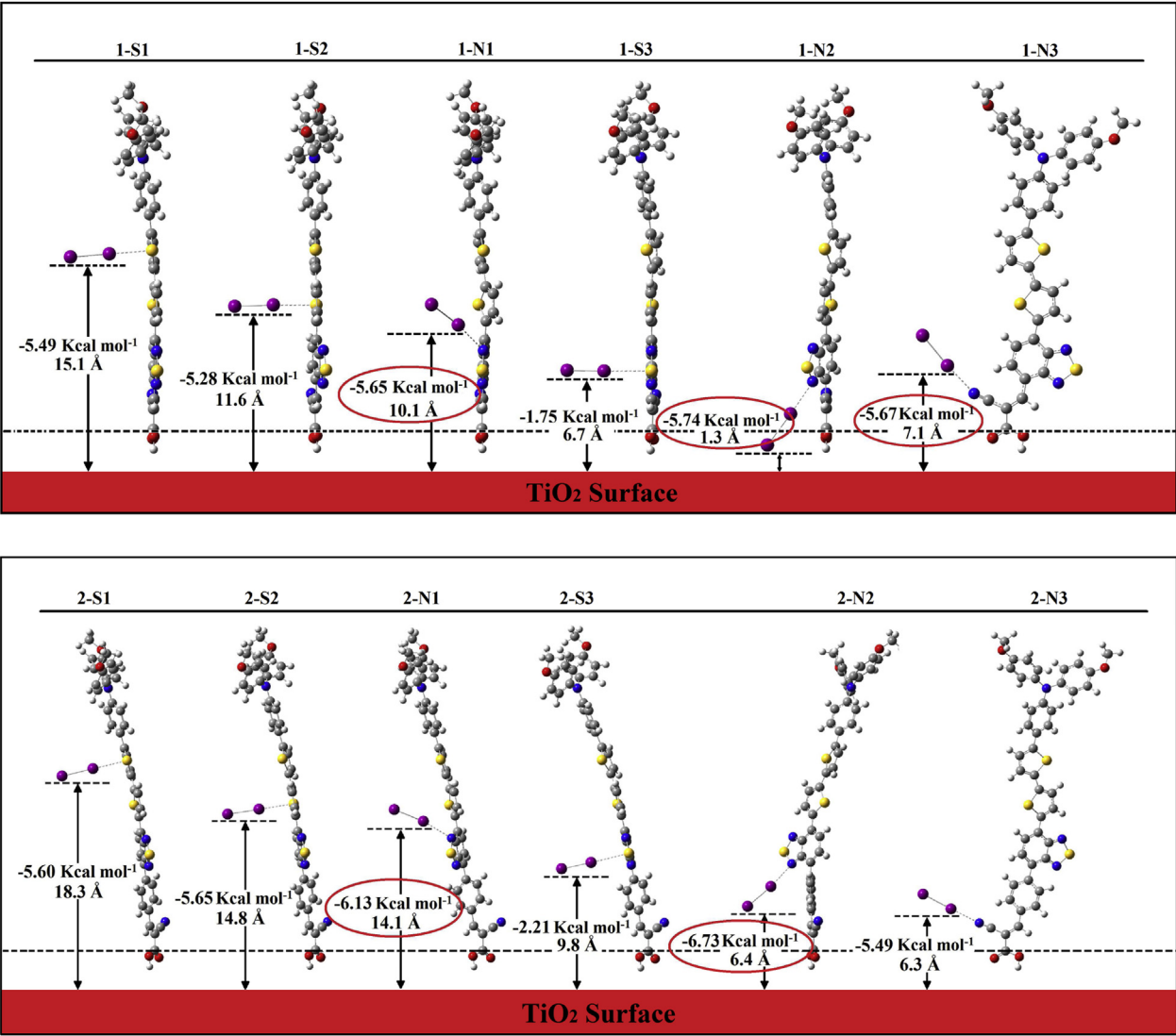


Fig. 5. The optimized molecular structures of dye-I₂ complexes for **1** and **2**.

were designed theoretically, taking **2** as a reference with the aim to further improve the performance of the sensitizer based on the following considerations: (i) since Wang et al. have demonstrated that the rigidification of bithiophene is an useful way to improve the light harvesting ability by increasing the molecular conjugation degree [55], **3** were designed; (ii) through our analysis, we realized that BTDA unit near the semiconductor surface could have a strong interaction with I₂, which could lead to the fast charge

Table 2
Computed maximum absorption wavelengths $\lambda_{\text{max}}/\text{nm}$ (eV) and nature of the transitions of **1** and **2** corresponding to $S_0 \rightarrow S_1$ in dichloromethane at TD-CPCM-CAM-B3LYP/6-31G(d) level with the B3LYP/6-31G(d) optimized geometries.

Dye	State	Main configuration ^a	$\lambda_{\text{max}}(\text{e}/\text{M}^{-1} \text{ cm}^{-1})^b$	$\lambda_{\text{max}}(\text{e}/\text{M}^{-1} \text{ cm}^{-1})^c$
1	$S_0 \rightarrow S_1$	H-1 \rightarrow L (0.38)	561(2.21)(27,129)	570(2.18)(18,900)
		H \rightarrow L (0.52)		
2	$S_0 \rightarrow S_1$	H-1 \rightarrow L (0.37)	501(2.47)(30,178)	515(2.41)(29,400)
		H \rightarrow L (0.43)		

^a H represents HOMO, L represents LUMO, and Data in parentheses are the main configuration contributions.
^b The molar absorption coefficients were simulated by Multiwfn.
^c Experimental values were obtained in dichloromethane from Ref. [34].

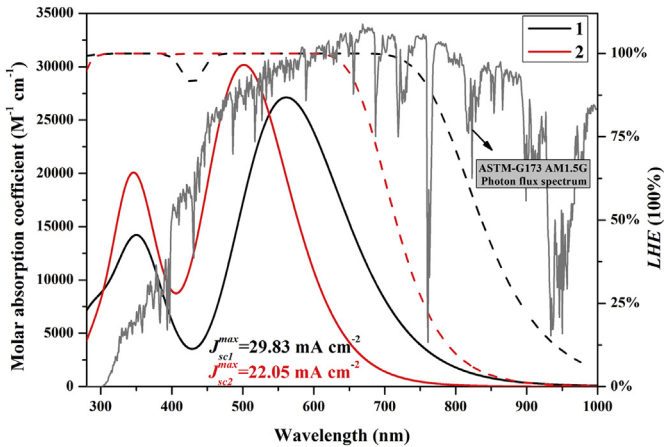


Fig. 6. The absorption spectra and LHE curves of **1** and **2** and their corresponding $J_{\text{sc}}^{\text{max}}$.

Table 3

Key parameters for deducing injection driving force (ΔG_{inj} /eV) and the corresponding experimental injection efficiencies.

Dye	E_{dye}/eV	λ_{max}	$E_{\text{dye}^+}/\text{eV}$	$\Delta G_{\text{inj}}/\text{eV}$	Φ_{inj}^a
1	−5.69	2.21	−3.48	0.52	94.8%
2	−5.58	2.47	−3.11	0.89	94.7%

^a Experimental values were obtained in dichloromethane from Ref. [34].

Table 4

Conduction band energy level shift ($\Delta\text{CB}/\text{eV}$), entity of charge transfer (q^{CT}/e), average electrostatic potential on the first layer of TiO_2 cluster (V_{EL}/eV), injection driving force ($\Delta G_{\text{inj}}/\text{eV}$), theoretical maximum limit of short circuit current density ($J_{\text{sc}}^{\text{max}}/\text{mA cm}^{-2}$), hole-surface distance ($r/\text{\AA}$) and position of predominant dye- I_2 interaction site for **2**–**7**.

	$\Delta\text{CB}/\text{eV}$	q^{CT}/e	V_{EL}/eV	$\Delta G_{\text{inj}}/\text{eV}$	$J_{\text{sc}}^{\text{max}}/\text{mA cm}^{-2}$	$r/\text{\AA}$	Position of predominant site (distance/ \AA) ^a
2	0.256	0.36	−0.21	0.89	5.293	19.9	2-N2 (6.4) 2-N1 (14.1)
3	0.241	0.37	−0.21	0.86	6.518	18.8	3-N1 (14.2) 3-N2 (6.7)
4	0.257	0.37	−0.21	0.77	6.000	18.6	4-S1 (18.6) 4-N1 (19.3) 4-N2 (12.3)
5	0.235	0.37	−0.21	0.95	6.625	22.1	5-N2 (6.8) 5-N3 (7.8) 5-N1 (14.9)
6	0.260	0.37	−0.21	0.81	8.517	20.3	6-N1 (19.4) 6-N2 (11.0)
7	0.240	0.38	−0.21	0.79	8.918	20.0	7-N2 (14.4) 7-N1 (23.6)

^a Data in parentheses are the corresponding approximate distance between I_2 and TiO_2 surface.

recombination process between the photoinjected electrons in the conduction band and the electrolyte, thus **4** with BTDA unit far away from the surface were designed; (iii) for **5**, the molecular length was increased by adding a thiophene ring aiming to further increase the hole-surface distance r , which is the main reason that contribute to the lower k_{rec1} of **2** compared to **1**. In a word, our aim of designing **3**–**5** is to further improve the advantages and avoid the disadvantages of **2**. Through our calculated results shown in Table 4 we found the desired properties were all presented in these three dyes. However, none of these three dyes are perfect due to some disadvantages. For instance, the dye cation hole-surface distance r of dyes **3** and **4** are 18.8 \AA and 18.6 \AA , which are slightly smaller than that of **2** (19.9 \AA), implying that their k_{rec1} will not be further retarded. For dye **5**, although its k_{rec1} has been reduced, there are more predominant interaction sites than that of **2** leading to a faster k_{rec1} . Thus, for designing more efficient dyes, we integrated these three molecular design principles into one leading to the design of **6** and **7** with just different conjugation order. The key parameters affecting the performance of both dyes compared with that of **2** discussed above are all collected in Table 4. From Table 4, the ΔG_{inj} of dyes **6** and **7** (0.81 eV and 0.79 eV respectively) are much larger than 0.2 eV, indicating that both dyes have enough injection driving force to inject electrons into the conduction band of semiconductor. Thus, we believe that both dyes have similar Φ_{inj} which are all close to one as well as **2**. And the corresponding ΔCBs of **6** and **7** are 0.260 eV and 0.240 eV, respectively, showing that dyes adsorbed onto TiO_2 could have noteworthy effect on conduction band energy level, leading to the increasing of V_{oc} . However, the difference among ΔCBs of **2**, **6** and **7** is so negligible that it can not bring significantly change on V_{oc} in this aspect. The calculated $J_{\text{sc}}^{\text{max}}$ of **6** and **7** are 32.40 mA cm^{-2} and 31.50 mA cm^{-2} respectively, implying that the theoretical maximum limit $J_{\text{sc}}^{\text{max}}$ of **6** and **7** are much larger

than that of **2** (22.05 mA cm^{-2}). The hole-surface distance r suggests that the cation holes of **6** and **7** are slightly farther than that of dye **2** implying that the k_{rec1} of both dyes are slightly smaller. With respect to k_{rec2} , although **6** and **7** have the same number of predominant interaction sites with **2**, all the predominant sites are farther than the corresponding ones in **2**. Thus, the k_{rec2} of **6** and **7** should also be smaller than that of **2**. As a consequence of the above, it is undoubtedly that both dyes we designed will be the promising candidates of DSSC.

4. Conclusions

The underlying origin of large efficiency difference for DSSCs based on dyes **1** and **2** with tiny structure difference was disclosed from the theoretical point of view. The parameters determining the efficiency of the cell, including ΔCB , n_c , $J_{\text{sc}}^{\text{max}}$, Φ_{inj} and η_{coll} were calculated through DFT and TDDFT calculations. The results show that although **2** has a little smaller theoretical maximum limit $J_{\text{sc}}^{\text{max}}$ than that of **1**, which is not beneficial for the enhancement of J_{sc} , the hole-surface distance r of **2** is larger and the predominant interaction site with I_2 is farther from the semiconductor surface due to the insertion of phenyl ring, which could lead to the slower charge recombination. Moreover, It gave us the hint that larger hole-surface distance r and the farther position of BTDA unit which has strong interaction with the I_2 could slow down the k_{rec} for the DSSC device. In this context, two dyes derived from **2** (**6** and **7**) with better conjugation degree, farther position of BTDA units and longer molecular length simultaneously were designed to further improve the performance of DSSCs. Fortunately, we find that we could get dyes with our desired properties through the reasonable rules, and **6** and **7** are the promising candidates in the DSSC field compared with **2**. We hope our work could provide a theoretical guidance for the future research of dye sensitized solar cell.

Acknowledgments

The authors gratefully acknowledge financial support from NSFC (21131001, 21273030, 21203019 and 21203020), SRFDP and RGC ERG Joint Research Program (20120043140001) and the Science and Technology Development Planning of Jilin Province (201201071 and 201201067). We are grateful to Computing Center of Jilin Province for essential support.

Appendix A. Supplementary data

Supplementary data related to this article can be found at <http://dx.doi.org/10.1016/j.jpowsour.2014.05.085>.

References

- [1] B. O'Regan, M. Grätzel, *Nature* 353 (1991) 737–740.
- [2] A. Hagfeldt, G. Boschloo, L. Sun, L. Kloo, H. Pettersson, *Chem. Rev.* 110 (2010) 6595–6663.
- [3] T. Kinoshita, J.T. Dy, S. Uchida, T. Kubo, H. Segawa, *Nat. Photon.* 7 (2013) 535–539.
- [4] J.H. Heo, S.H. Im, J.H. Noh, T.N. Mandal, C.S. Lim, J.A. Chang, Y.H. Lee, H.J. Kim, A. Sarkar, M.K. Nazeeruddin, M. Grätzel, S.I. Seok, *Nat. Photon.* 7 (2013) 486–491.
- [5] I. Chung, B. Lee, J. He, R.P.H. Chang, M.G. Kanatzidis, *Nature* 485 (2012) 486–489.
- [6] S. Zhang, X. Yang, Y. Numata, L. Han, *Energy Environ. Sci.* 6 (2013) 1443–1464.
- [7] S. Mathew, A. Yella, P. Gao, R. Humphry-Baker, F.E. Curchod, N. Ashari-Astani, I. Tavernelli, U. Rothlisberger, K. Nazeeruddin, M. Grätzel, *Nat. Chem.* 6 (2014) 242–247.
- [8] A. Yella, H.W. Lee, H.N. Tsao, C. Yi, A.K. Chandiran, M.K. Nazeeruddin, E.W.G. Diau, C.Y. Yeh, S.M. Zakeeruddin, M. Grätzel, *Science* 334 (2011) 629–634.
- [9] M. Taguchi, A. Yano, S. Tohoda, K. Matsuyama, Y. Nakamura, T. Nishiwaki, K. Fujita, E. Maruyama, *Photovolt. IEEE J.* 4 (2014) 96–99.

- [10] H. Tsubomura, M. Matsumura, Y. Nomura, T. Amamiya, *Nature* 261 (1976) 402–403.
- [11] T. Bessho, S.M. Zakeeruddin, C.Y. Yeh, E.W.G. Diao, M. Grätzel, *Angew. Chem. Int. Ed.* 49 (2010) 6646–6649.
- [12] F. Sauvage, J.D. Decoppet, M. Zhang, S.M. Zakeeruddin, P. Comte, M. Nazeeruddin, P. Wang, M. Grätzel, *J. Am. Chem. Soc.* 133 (2011) 9304–9310.
- [13] M.K. Nazeeruddin, F. De Angelis, S. Fantacci, A. Selloni, G. Viscardi, P. Liska, S. Ito, B. Takeru, M. Grätzel, *J. Am. Chem. Soc.* 127 (2005) 16835–16847.
- [14] J. Burschka, N. Pellet, S.-J. Moon, R. Humphry-Baker, P. Gao, M.K. Nazeeruddin, M. Grätzel, *Nature* 499 (2013) 316–319.
- [15] P. Péchy, T. Renouard, S.M. Zakeeruddin, R. Humphry-Baker, P. Comte, P. Liska, L. Cevey, E. Costa, V. Shklover, L. Spiccia, G.B. Deacon, C.A. Bignozzi, M. Grätzel, *J. Am. Chem. Soc.* 123 (2001) 1613–1624.
- [16] M.K. Nazeeruddin, A. Kay, I. Rodicio, R. Humphry-Baker, E. Mueller, P. Liska, N. Vlachopoulos, M. Grätzel, *J. Am. Chem. Soc.* 115 (1993) 6382–6390.
- [17] M.K. Nazeeruddin, S.M. Zakeeruddin, R. Humphry-Baker, M. Jirousek, P. Liska, N. Vlachopoulos, V. Shklover, C.-H. Fischer, M. Grätzel, *Inorg. Chem.* 38 (1999) 6298–6305.
- [18] Q. Yu, Y. Wang, Z. Yi, N. Zu, J. Zhang, M. Zhang, P. Wang, *ACS Nano* 4 (2010) 6032–6038.
- [19] Y.-C. Chang, C.-L. Wang, T.-Y. Pan, S.-H. Hong, C.-M. Lan, H.-H. Kuo, C.-F. Lo, H.-Y. Hsu, C.-Y. Lin, E.W.-G. Diao, *Chem. Commun.* 47 (2011) 8910–8912.
- [20] S.-L. Wu, H.-P. Lu, H.-T. Yu, S.-H. Chuang, C.-L. Chiu, C.-W. Lee, E.W.-G. Diao, C.-Y. Yeh, *Energy Environ. Sci.* 3 (2010) 949–955.
- [21] A. Mishra, M.K.R. Fischer, P. Bäuerle, *Angew. Chem. Int. Ed.* 48 (2009) 2474–2499.
- [22] L.-Y. Lin, C.-P. Lee, M.-H. Yeh, A. Baheti, R. Vittal, K.R.J. Thomas, K.-C. Ho, *J. Power Sources* 215 (2012) 122–129.
- [23] L.-Y. Lin, M.-H. Yeh, C.-P. Lee, J. Chang, A. Baheti, R. Vittal, K.R. Justin Thomas, K.-C. Ho, *J. Power Sources* 247 (2014) 906–914.
- [24] W. Zeng, Y. Cao, Y. Bai, Y. Wang, Y. Shi, M. Zhang, F. Wang, C. Pan, P. Wang, *Chem. Mater.* 22 (2010) 1915–1925.
- [25] M. Pastore, E. Mosconi, F. De Angelis, *J. Phys. Chem. C* 116 (2012) 5965–5973.
- [26] S.L. Chen, L.N. Yang, Z.S. Li, *J. Power Sources* 223 (2013) 86–93.
- [27] X.S. Liu, Z.C. Cao, H.L. Huang, X.X. Liu, Y.Z. Tan, H.J. Chen, Y. Pei, S.T. Tan, *J. Power Sources* 248 (2014) 400–406.
- [28] Y. Hua, B. Jin, H.D. Wang, X.J. Zhu, W.J. Wu, M.S. Cheung, Z.Y. Lin, W.Y. Wong, W.K. Wong, *J. Power Sources* 237 (2013) 195–203.
- [29] N. Cai, J. Zhang, M. Xu, M. Zhang, P. Wang, *Adv. Funct. Mater.* 23 (2013) 3539–3547.
- [30] A. Yella, R. Humphry-Baker, B.F.E. Curchod, N. Ashari Astani, J. Teuscher, L.E. Polander, S. Mathew, J.E. Moser, I. Tavernelli, U. Rothlisberger, M. Grätzel, M.K. Nazeeruddin, J. Frey, *Chem. Mater.* 25 (2013) 2733–2739.
- [31] W.H. Nguyen, C.D. Bailie, J. Burschka, T. Moehl, M. Grätzel, M.D. McGehee, A. Sellinger, *Chem. Mater.* 25 (2013) 1519–1525.
- [32] J. Feng, Y. Jiao, W. Ma, M.K. Nazeeruddin, M. Grätzel, S. Meng, *J. Phys. Chem. C* 117 (2013) 3772–3778.
- [33] J.H. Delcamp, A. Yella, T.W. Holcombe, M.K. Nazeeruddin, M. Grätzel, *Angew. Chem. Int. Ed.* 52 (2013) 376–380.
- [34] S. Haid, M. Marszalek, A. Mishra, M. Wielopolski, J. Teuscher, J.E. Moser, R. Humphry-Baker, S.M. Zakeeruddin, M. Grätzel, P. Bäuerle, *Adv. Funct. Mater.* 22 (2012) 1291–1302.
- [35] M.J. Frisch, G.W. Trucks, H.B. Schlegel, G.E. Scuseria, M.A. Robb, J.R. Cheeseman, G. Scalmani, V. Barone, B. Mennucci, G.A. Petersson, H. Nakatsuji, M. Caricato, X. Li, H.P. Hratchian, A.F. Izmaylov, J. Bloino, G. Zheng, J.L. Sonnenberg, M. Hada, M. Ehara, K. Toyota, R. Fukuda, J. Hasegawa, M. Ishida, T. Nakajima, Y. Honda, O. Kitao, H. Nakai, T. Vreven, J.J.A. Montgomery, J.E. Peralta, F. Ogliaro, M. Bearpark, J.J. Heyd, E. Brothers, K.N. Kudin, V.N. Staroverov, R. Kobayashi, J. Normand, K. Raghavachari, A. Rendell, J.C. Burant, S.S. Iyengar, J. Tomasi, M. Cossi, N. Rega, J.M. Millam, M. Klene, J.E. Knox, J.B. Cross, V. Bakken, C. Adamo, J. Jaramillo, R. Gomperts, R.E. Stratmann, O. Yazyev, A.J. Austin, R. Cammi, C. Pomelli, J.W. Ochterski, R.L. Martin, K. Morokuma, V.G. Zakrzewski, G.A. Voth, P. Salvador, J.J. Dannenberg, S. Dapprich, A.D. Daniels, O. Farkas, J.B. Foresman, J.V. Ortiz, J. Cioslowski, D.J. Fox, *Gaussian 09W, Revision A.02*, Gaussian, Inc., Wallingford CT, 2009.
- [36] J. Preat, C. Michaux, D. Jacquemin, E.A. Perpete, *J. Phys. Chem. C* 113 (2009) 16821–16833.
- [37] V. Barone, M. Cossi, *J. Phys. Chem. A* 102 (1998) 1995–2001.
- [38] T. Yanai, D.P. Tew, N.C. Handy, *Chem. Phys. Lett.* 393 (2004) 51–57.
- [39] Y. Zhao, D. Truhlar, *Theor. Chem. Acc.* 120 (2008) 215–241.
- [40] Y. Zhao, D.G. Truhlar, *Acc. Chem. Res.* 41 (2008) 157–167.
- [41] K.E. Riley, M. Pitoňák, P. Jurečka, P. Hobza, *Chem. Rev.* 110 (2010) 5023–5063.
- [42] S.F. Boys, F. Bernardi, *Mol. Phys.* 19 (1970) 553–566.
- [43] M.D. Newton, N.R. Kestner, *Chem. Phys. Lett.* 94 (1983) 198–201.
- [44] P. Persson, R. Bergström, S. Lunell, *J. Phys. Chem. B* 104 (2000) 10348–10351.
- [45] A. Vittadini, A. Selloni, F.P. Rotzinger, M. Grätzel, *J. Phys. Chem. B* 104 (2000) 1300–1306.
- [46] S.D. Burnside, V. Shklover, C. Barbé, P. Comte, F. Arendse, K. Brooks, M. Grätzel, *Chem. Mater.* 10 (1998) 2419–2425.
- [47] F. De Angelis, A. Tilocca, A. Selloni, *J. Am. Chem. Soc.* 126 (2004) 15024–15025.
- [48] F. De Angelis, *Chem. Phys. Lett.* 493 (2010) 323–327.
- [49] P. Ordejón, E. Artacho, J.M. Soler, *Phys. Rev. B Condens. Matter Phys.* 53 (1996) R10441–R10444.
- [50] M.S. José, A. Emilio, D.G. Julian, G. Alberto, J. Javier, O. Pablo, S.P. Daniel, *J. Phys. Condens. Matter* 14 (2002) 2745–2779.
- [51] D. Sánchez-Portal, P. Ordejón, E. Artacho, J.M. Soler, *Int. J. Quantum Chem.* 65 (1997) 453–461.
- [52] M. Cossi, *J. Chem. Phys.* 115 (2001) 4708–4717.
- [53] M. Grätzel, *Acc. Chem. Res.* 42 (2009) 1788–1798.
- [54] T. Marinado, K. Nonomura, J. Nissfolk, M.K. Karlsson, D.P. Hagberg, L. Sun, S. Mori, A. Hagfeldt, *Langmuir* 26 (2009) 2592–2598.
- [55] M. Xu, M. Zhang, M. Pastore, R. Li, F. De Angelis, P. Wang, *Chem. Sci.* 3 (2012) 976–983.
- [56] E. Ronca, M. Pastore, L. Belpassi, F. Tarantelli, F. De Angelis, *Energy Environ. Sci.* 6 (2013) 183–193.
- [57] J. Zhang, Y.H. Kan, H.B. Li, Y. Geng, Y. Wu, Z.M. Su, *Dyes Pigm.* 95 (2012) 313–321.
- [58] J. Zhang, H.B. Li, J.Z. Zhang, Y. Wu, Y. Geng, Q. Fu, Z.M. Su, *J. Mater. Chem. A* 1 (2013) 14000–14007.
- [59] Y. Jiao, F. Zhang, M. Grätzel, S. Meng, *Adv. Funct. Mater.* 23 (2013) 424–429.
- [60] M. Planells, L. Pelleja, J.N. Clifford, M. Pastore, F. De Angelis, N. Lopez, S.R. Marder, E. Palomares, *Energy Environ. Sci.* 4 (2011) 1820–1829.
- [61] H. Gerischer, *Z. Phys. Chem.* 26 (1960) 223–247.
- [62] H. Gerischer, *Adv. Electroch. EL. Eng.* 1 (1961) 139–232.
- [63] H. Gerischer, M.E. Michel-Beyerle, F. Rebertus, H. Tributsch, *Electrochim. Acta* 13 (1968) 1509–1515.
- [64] J.N. Clifford, E. Palomares, M.K. Nazeeruddin, M. Grätzel, J. Nelson, X. Li, N.J. Long, J.R. Durrant, *J. Am. Chem. Soc.* 126 (2004) 5225–5233.
- [65] T. Clark, M. Hennemann, J. Murray, P. Politzer, *J. Mol. Model.* 13 (2007) 291–296.
- [66] P. Politzer, P. Lane, M. Concha, Y. Ma, J. Murray, *J. Mol. Model.* 13 (2007) 305–311.
- [67] T. Clark, *WIREs Comput. Mol. Sci.* 3 (2013) 13–20.
- [68] Y. Bai, J. Zhang, D. Zhou, Y. Wang, M. Zhang, P. Wang, *J. Am. Chem. Soc.* 133 (2011) 11442–11445.
- [69] B.C. O'Regan, J.R. Durrant, *Acc. Chem. Res.* 42 (2009) 1799–1808.
- [70] M. Tuikka, P. Hirva, K. Rissanen, J. Korppi-Tommola, M. Haukka, *Chem. Commun.* 47 (2011) 4499–4501.
- [71] B.C. O'Regan, K. Walley, M. Juozapavicius, A. Anderson, F. Matar, T. Ghaddar, S.M. Zakeeruddin, C.D. Klein, J.R. Durrant, *J. Am. Chem. Soc.* 131 (2009) 3541–3548.
- [72] M. Miyashita, K. Sunahara, T. Nishikawa, Y. Uemura, N. Koumura, K. Hara, A. Mori, T. Abe, E. Suzuki, S. Mori, *J. Am. Chem. Soc.* 130 (2008) 17874–17881.
- [73] J. Zhang, H.B. Li, Y. Geng, S.Z. Wen, R.L. Zhong, Y. Wu, Q. Fu, Z.M. Su, *Dyes Pigm.* 99 (2013) 127–135.
- [74] Z.S. Wang, K. Hara, Y. Dan-oh, C. Kasada, A. Shinpo, S. Suga, H. Arakawa, H. Sugihara, *J. Phys. Chem. B* 109 (2005) 3907–3914.
- [75] K. Srinivas, K. Yesudas, K. Bhanuprakash, V.J. Rao, L. Giribabu, *J. Phys. Chem. C* 113 (2009) 20117–20126.
- [76] A.N.M. Green, R.E. Chandler, S.A. Haque, J. Nelson, J.R. Durrant, *J. Phys. Chem. B* 109 (2004) 142–150.
- [77] C.E. Richards, A.Y. Anderson, S. Martiniani, C. Law, B.C. O'Regan, *J. Phys. Chem. Lett.* 3 (2012) 1980–1984.
- [78] A.V. Akimov, A.J. Neukirch, O.V. Prezhdo, *Chem. Rev.* 113 (2013) 4496–4565.
- [79] S. Ardo, G.J. Meyer, *Chem. Soc. Rev.* 38 (2009) 115–164.
- [80] G.M. Hasselman, D.F. Watson, J.R. Stromberg, D.F. Bocian, D. Holten, J.S. Lindsey, G.J. Meyer, *J. Phys. Chem. B* 110 (2006) 25430–25440.
- [81] W. Ma, Y. Jiao, S. Meng, *J. Phys. Chem. C* (2014), <http://dx.doi.org/10.1021/jp410982e>.
- [82] Y. Jiao, W. Ma, S. Meng, *Chem. Phys. Lett.* 586 (2013) 97–99.
- [83] J. Zhang, H.B. Li, S.L. Sun, Y. Geng, Y. Wu, Z.M. Su, *J. Mater. Chem.* 22 (2012) 568–576.
- [84] J. Wang, F.Q. Bai, B.H. Xia, L. Feng, H.X. Zhang, Q.J. Pan, *Phys. Chem. Chem. Phys.* 13 (2011) 2206–2213.
- [85] J. Zhang, Y.H. Kan, H.B. Li, Y. Geng, Y. Wu, Y.A. Duan, Z.M. Su, *J. Mol. Model.* 19 (2013) 1597–1604.
- [86] M. Grätzel, *Nature* 414 (2001) 338–344.
- [87] T. Lu, F. Chen, *J. Comput. Chem.* 33 (2012) 580–592.
- [88] T. Lu Multiwfn, Version 3.2, A Multifunctional Wavefunction Analyzer, see <http://multiwfn.codeplex.com>.
- [89] A. Islam, H. Sugihara, H. Arakawa, *J. Photochem. Photobiol. A* 158 (2003) 131–138.